



31 phosphorus ( $\text{PO}_4^{3-}$ ), methane ( $\text{CH}_4$ ), carbon dioxide ( $\text{CO}_2$ ) and nitrous oxide ( $\text{N}_2\text{O}$ ). In  
32 this study, laboratory-scale denitrifying bioreactors operated at hydraulic retention  
33 times (HRTs) ranging from 4 to 22 d, containing either lodgepole pine woodchips  
34 (LPW), lodgepole pine needles (LPN), barley straw (BBS) or cardboard, were  
35 investigated to elucidate operational optima considering three scenarios using: (1)  
36 only  $\text{NO}_3^-$  net fluxes (2)  $\text{NO}_3^-$ ,  $\text{NH}_4^+$  and  $\text{PO}_4^{3-}$  combined fluxes (3) all fluxes (water  
37 and gaseous) combined. At the end of the experiment, after up to 745 days of  
38 operation, the bioreactors were destructively sampled for microbial analysis. In  
39 Scenario 1, there was a net removal in the bioreactors, which generally performed  
40 best at shorter HRTs. In Scenario 2, there was a net release of contaminants from all  
41 bioreactors, which substantially increased in Scenario 3. Total greenhouse gas  
42 emissions were highest for the cardboard bioreactors ( $296 \text{ g CO}_2\text{-eq m}^{-2} \text{ d}^{-1}$ ) at the  
43 longest HRT, and were dominated by  $\text{CH}_4$  emissions. Highest  $\text{N}_2\text{O}$  emissions  
44 emanated from LPN and LPW bioreactors, which also had a greater proportion of  
45 denitrifiers than the other bioreactors. Overall, considering all three scenarios, LPN  
46 bioreactors were the best performing at all HRTs. However, the long-term availability  
47 of its carbon source may be limited, as there was an 80% reduction over a 560 d  
48 period.

49

50 *Keywords:* Denitrification; denitrification bioreactors; greenhouse gas emissions;  
51 pollution swapping.

52

53 **1. Introduction**

54

55 Excess reactive nitrogen, such as nitrate ( $\text{NO}_3^-$ ), ammonium ( $\text{NH}_4^+$ ) or nitrous oxide  
56 ( $\text{N}_2\text{O}$ ) are now at levels which contribute to eutrophication of terrestrial and aquatic  
57 ecosystems (Flecharth *et al.*, 2011) and climate change (Richardson *et al.*, 2009). In  
58 Europe, nitrogen (N) concentrations in rivers, lakes, aquifers and coastal regions are  
59 high in some regions, and groundwater  $\text{NO}_3^-$  concentrations are generally on the  
60 increase (Grizzetti *et al.*, 2012). Residence times of pollutants migrating through soil,  
61 subsoil and aquifers can be from months (e.g. well drained and high permeability) to  
62 years (e.g. moderately drained and low permeability) (Fenton *et al.*, 2011), leading to  
63 sustained losses of  $\text{NO}_3^-$  to surface water and indirect  $\text{N}_2\text{O}$  emissions to the  
64 atmosphere in areas where only partial denitrification occurs (e.g. areas of high water  
65 velocity, high dissolved oxygen (DO) concentrations, or low dissolved organic carbon  
66 (DOC) concentrations; Durand *et al.*, 2011). The carbon (C) and N cycles are  
67 intrinsically linked and depend heavily on the dynamic development of in situ  
68 microbial communities, which transform these communities via different pathways.

69

70 Denitrification bioreactors containing organic C rich media, located where  
71 denitrification potentials are low and  $\text{NO}_3^-$  concentrations are high (e.g. drainage tiles  
72 or outlets of artificial and natural drainage networks such as pipe and spring outlets),  
73 may enhance microbial reduction of  $\text{NO}_3^-$  by converting it to  $\text{N}_2$  (Schipper *et al.*,  
74 2010). Bioreactor design, and in particular hydraulic retention time (HRT), is  
75 therefore important to facilitate full denitrification, and can be used as a tool to  
76 control indirect emissions of  $\text{N}_2\text{O}$  (Fujinuma *et al.*, 2011). These indirect emissions,  
77 which may also include losses of other greenhouse gases (GHGs) such as methane  
78 ( $\text{CH}_4$ ) and carbon dioxide ( $\text{CO}_2$ ), as well as  $\text{NH}_4^+$ , phosphorus (P), organic C and  
79 metals, is referred to as ‘pollution swapping’ (Fenton *et al.*, 2014). Relatively few

80 studies have considered pollution swapping in the evaluation of denitrification  
81 bioreactors (Grennan *et al.*, 2009; Elgood *et al.*, 2010; Warneke *et al.*, 2011a).  
82 However, no study has yet attempted to develop a metric to evaluate the performance  
83 of bioreactors containing different C-rich media, which considers pollution swapping  
84 across a range of HRTs, and the community of denitrifying microorganisms  
85 supporting this community.

86

87 Optimal  $\text{NO}_3^-$  removal rates ( $\text{g NO}_3\text{-N m}^{-3} \text{d}^{-1}$ ) depend on factors such as reactive  
88 media type, C concentration and bioavailability (Cameron and Schipper, 2010),  
89 temperature (Warneke *et al.*, 2011a); hydraulic, DO and  $\text{NO}_3^-$  loading rates (Grennan  
90 *et al.*, 2009; Xu *et al.*, 2009), and HRTs (Chun *et al.*, 2009; Christianson *et al.*, 2011).  
91 Typically, optimal N removal rates are determined by operating a bioreactor system  
92 under various  $\text{NO}_3^-$  loading rates (Healy *et al.*, 2006). Fenton *et al.* (2009) found a  
93 direct negative relationship between denitrification potential in shallow groundwater  
94 and saturated hydraulic conductivity ( $k_s$ ) of subsoil. Consequently, even if optimal  
95 conditions for denitrification exist (Rivett *et al.*, 2008), microbially-mediated  
96 reactions may be limited when  $k_s$ , or hydraulic gradients, are too high.

97

98 There has been little work on the impact of different C sources on the abundance of  
99 the microbial community catalysing  $\text{NO}_3^-$  removal in denitrifying bioreactors (e.g.,  
100 Moorman *et al.*, 2010; Warneke *et al.*, 2011b). Warneke *et al.* (2011b) examined this  
101 by measuring the functional gene copy numbers for nitrite reductase, *nirS* and *nirK*,  
102 and nitrous-oxide reductase, *nosZ*, for different C substrates, including woodchips,  
103 sawdust, green waste, maize cobs and wheat straw, in laboratory bioreactors operated  
104 at different temperatures (16.8 and 27.1°C). They found that microbially-mediated

105 denitrification was the main mechanism for  $\text{NO}_3^-$ -N removal, the abundance of  
106 denitrifying genes was similar in all bioreactors operated at the lower temperature,  
107 and that  $\text{NO}_3^-$ -N removal was mainly limited by C availability and temperature. No  
108 study has yet investigated the development of denitrifying community abundance with  
109 respect to distance from the inlet in a denitrifying bioreactor.

110

111 The objectives of this study were to: (1) investigate the relationship between  $\text{NO}_3^-$   
112 removal and pollution swapping during successive, incrementally decreasing HRTs  
113 in denitrification bioreactors containing different C-rich media (lodgepole woodchips  
114 (LPW), lodgepole pine needles (LPN), barley straw (BBS) and cardboard); (2)  
115 identify optimum HRTs for each media, in which acceptable  $\text{NO}_3^-$  treatment can be  
116 achieved, while minimising other losses; (3) examine whether the source of carbon in  
117 a bioreactor influences the abundance of the functional genes *nirK*, *nirS* and *nosZ*.

118

## 119 **2. Materials and Methods**

120

### 121 **2.1 Operation of bioreactors**

122

123 The laboratory bioreactors of Healy *et al.* (2012) were used in the current study.  
124 Briefly, these were 0.1 m-diameter x 1 m-long acrylic columns, which were loaded at  
125 the base to allow even saturation and uniform flow into each column. They contained  
126 either LPW, cardboard, LPN, or BBS (all at n=3), mixed in alternating 0.03 m-thick  
127 layers with soil to give a C source-to-soil volume ratio of 1. Prior to operation, each  
128 bioreactor was seeded with approximately 1 L of bulk fluid from a wastewater  
129 treatment plant. This fluid was applied to the surface of each bioreactor and allowed

130 to percolate through the media. A control bioreactor (n=2), containing soil only  
131 (CSO) was also included. The LPW and cardboard bioreactors were operated to  
132 determine their long-term performance. In the Healy *et al.* (2012) study, all  
133 bioreactors were loaded with  $\text{NO}_3^-$ -N solution varying from 19.5 to 32.5  $\text{mg L}^{-1}$  at a  
134 hydraulic loading rate (HLR) of 3  $\text{cm d}^{-1}$ .

135

136 In the current study, the bioreactors were operated at incrementally increasing HLRs  
137 of 5 and 10  $\text{cm d}^{-1}$  (Table 1) and the influent  $\text{NO}_3^-$ -N concentration was varied from  
138 20 to 29.6  $\text{mg L}^{-1}$  over both loading rates. A conservative tracer (NaBr, 10  $\text{g L}^{-1}$ ,  
139 applied in one pulse in one constant hydraulic loading interval) was used to estimate  
140 the average HRT within each bioreactor, at each HLR, after Levenspiel (1999).

141

## 142 **2.2 Water analysis**

143

144 Water samples collected at the inlet, outlet and at three sampling ports (SPs), located  
145 at distances of 0.2 (SP1), 0.4 (SP2) and 0.6 m (SP3) from the inlet of each column,  
146 were analysed using standard methods (APHA, 1995) for  $\text{NO}_3^-$ -N,  $\text{NH}_4^+$ -N, nitrite-N  
147 ( $\text{NO}_2^-$ -N), ortho-phosphorus ( $\text{PO}_4^{3-}$ -P), chemical oxygen demand (COD), pH and DO.

148 Nitrate removal rates (NR;  $\text{g NO}_3^-$ -N  $\text{m}^{-3} \text{d}^{-1}$ ) were calculated taking into account the  
149 Darcy velocity ( $q$ ,  $\text{m d}^{-1}$ ), cross sectional area ( $A$ ,  $\text{m}^2$ ), volume of the active area of the  
150 bioreactors ( $\text{m}^3$ ), and change in  $\text{NO}_3^-$ -N concentration from the inlet to outlet ( $\Delta[\text{NO}_3^-$   
151  $-N]$ ,  $\text{g m}^{-3}$ ):

152

$$153 \quad NR = \frac{q \times A \times \Delta[\text{NO}_3^- - N]}{\text{media volume}} \quad (\text{g NO}_3^- \text{-N m}^{-3} \text{d}^{-1}) \quad [1]$$

154

### 155 **2.3 Greenhouse gas analysis**

156

157 The emission of GHG, comprising CO<sub>2</sub>, CH<sub>4</sub> and N<sub>2</sub>O, from each column was  
158 measured at specific times at each HLR using the static chamber technique  
159 (Hutchinson and Mosier, 1981). The headspace above each column was flushed with  
160 argon (Ar) gas for 5 min at a flow rate of 3 L min<sup>-1</sup>. Gas samples were withdrawn at 0,  
161 15 and 30 min, and samples were analysed using a gas chromatograph (GC) (Varian  
162 GC 450; The Netherlands) and automatic sampler (Combi-PAL autosampler; CTC  
163 Analytics, Zwingen, Switzerland). Fluxes of CO<sub>2</sub>, CH<sub>4</sub> and N<sub>2</sub>O for each chamber  
164 were measured as a function of headspace gas accumulation over time (Hutchinson  
165 and Mosier, 1981). Data analyses were performed on average daily and cumulative  
166 emissions by ANOVA, using the PROC GLM procedure of SAS (SAS Institute, Cary,  
167 NC, 2003) with *post-hoc* least significant differences (LSD) tests used to identify  
168 differences between treatments.

169

### 170 **2.4 Carbon, nitrogen and phosphorus analysis of soil and media**

171

172 Before construction of the bioreactors, the C and N content of all C-rich media and  
173 soil were determined using a thermal conductivity detector, following combustion and  
174 separation in a chromatographic column, and the P content was determined by  
175 inductively coupled plasma emission spectroscopy (ICP-ES) after aqua regia  
176 digestion. As the C-rich media were placed in the bioreactors in alternating 0.03 m-  
177 thick layers with soil and the total mass within each reactor was measured, the initial  
178 C and N content, expressed as %w/w, and the P content, expressed as mg kg<sup>-1</sup> (dry

179 matter), in each bioreactor could be calculated. Upon completion of the experiment,  
180 two denitrifying bioreactors from each treatment were destructively sampled and  
181 samples from four sections, each 0.2 m in length, of each bioreactor (inlet to SP1, SP1  
182 to SP2, SP2 to SP3, SP3 to SP4) were analysed for C, N and P content. This enabled  
183 the relationship between total C loss within each bioreactor and the cumulative COD  
184 loss, the C content of the bioreactors, and the loss of P to be deduced for the period of  
185 operation.

186

### 187 **2.5 DNA extraction and real-time PCR analysis on the media**

188

189 Real time PCR was used to quantify the archaeal and bacterial 16S rRNA populations  
190 present in each bioreactor, as well as populations of denitrifying microorganisms  
191 using the denitrifying genes, *nirK*, *nirS* and *nosZ* (Table 2). Archaeal and bacterial  
192 16S rRNA populations were distinguished by using two sets of primers and specific  
193 probes for each group. Results are described as gene copy concentrations per gram of  
194 soil (GCCs/GCs g<sub>[soil]</sub><sup>-1</sup>).

195

196 Soil used for microbiological analysis was sampled from each 0.2-m-length of each  
197 column (inlet to SP1, SP1 to SP2, SP2 to SP3, SP3 to SP4), and the genomic DNA  
198 was extracted from 0.5 g/ soil using the UltraClean™ Soil DNA Isolation kit  
199 following the manufacturer's guidelines. The extracted genomic DNA was visualized  
200 on 1% (w/v) 1X TAE agarose gels and was quantified using the Nanodrop 2000c  
201 spectrophotometer (Thermo Scientific Inc). Extracted DNA was then stored at -20°C.

202

203 Standard curves for absolute quantification of archaeal and bacterial 16S rRNA genes  
204 and the *nirS*, *nirK* and *nosZ* denitrification genes were constructed using the  
205 corresponding standard strains and primer/probe sets outlined in Barrett *et al.* (2013;  
206 Table 2). Briefly, a 10-fold dilution series of each standard plasmid solution was  
207 prepared and analysed using the Light Cycler 480 (Roche, Mannheim, Germany);  
208 real-time PCR was carried out in duplicate employing the corresponding primer/probe  
209 set outlined in Yu *et al.* (2005) and Barrett *et al.* (2013). For the archaeal 16S rRNA  
210 gene, an equimolar mixture of the corresponding standard plasmids was used as the  
211 template solution for construction of the standard curve (Yu *et al.*, 2005; Lee *et al.*,  
212 2009). Bacterial and archaeal 16S rRNA genes were analysed in duplicate using the  
213 Light Cycler 480 (Roche, Mannheim, Germany), the LightCycler 480 Taqman  
214 hydrolysis probe Master kit (Roche), and the corresponding primer/probe sets and  
215 LightCycler 480 Probe Master kit (Roche; Table 2). The *nirK*, *nirS* and *nosZ* genes  
216 were analysed using the corresponding primer sets with the LightCycler 480 SYBR  
217 Green I Master kit (Roche), in a total volume of 20  $\mu$ l, according to the  
218 manufacturer's instructions (Yu *et al.*, 2005; Barrett *et al.*, 2013). The thermal cycling  
219 protocol was as outlined in Braker *et al.* (1998), Kandeler *et al.* (2006) and Henry *et*  
220 *al.* (2006).

221

222 Changes in gene copy number between all samples generated from replicate  
223 bioreactors and sampling ports using alternative C sources were analysed with one-  
224 way ANOVA, followed by the *post-hoc* Tukey test (Graph Pad InStat V3). Individual  
225 regression analysis of *nirK* and *nirS* gene copy number versus N<sub>2</sub>O as for *nosZ* and N<sub>2</sub>  
226 were also carried out using Graph Pad InStat V3. Using Primer v6 (Primer-E,  
227 Plymouth, UK), a Bray-Curtis resemblance matrix (Clarke *et al.*, 2006) was generated

228 for each bioreactor and sampling port using square root transformed mean 16S rRNA,  
229 *nirS*, *nirK* and *nosZ* gene copy abundances. Using the resultant resemblance matrix,  
230 the data were analyzed in a group average hierarchical cluster dendrogram.

231

## 232 **2.6 Sustainability Index**

233

234 Fenton *et al.* (2014) developed a simple method to quantify the effectiveness of  
235 denitrification bioreactors, which considered ‘pollution swapping’. In this method, the  
236 removal or production of each measured parameter is considered separately. To create  
237 equivalence between water and gas measurements, all parameters are expressed in g  
238 m<sup>-2</sup> (of bioreactor surface area) d<sup>-1</sup> and the GHGs are expressed in CO<sub>2</sub> equivalents to  
239 account for global warming potential. Negative and positive balances of each  
240 parameter indicate either removal or production of the parameter of interest. A  
241 sustainability index (SI) is then created by adding each of these parameters together,  
242 after Fenton *et al.* (2014):

243

$$244 \quad SI = a(B_{N_2O}) + b(B_{NO_3^-}) + c(B_{CH_4}) + d(B_{CO_2}) + etc..... \quad [2]$$

245

246 where  $B_x$  denotes the net flux (either positive or negative) of a specific parameter ( $x$ )  
247 from the denitrification bioreactor, and  $a$ ,  $b$ ,  $c$ , etc. are weighting factors that depend  
248 on the context of the analysis (e.g. legislative, environmental, geographical). For  
249 example, if  $NO_3^-$  was considered the most important parameter, the weighting factor  $b$   
250 in Eqn. 2 would be set at 1 and all other parameters would be less than 1. Three  
251 simple scenarios are considered in this study - Scenario 1: In countries where  $NO_3^-$   
252 removal is of most interest and GHG emissions to the atmosphere are perceived as

253 secondary, the weighting factor for  $\text{NO}_3^-$  is set to 1 and those for the other measured  
254 parameters ( $\text{NH}_4^+\text{-N}$ ,  $\text{PO}_4^{3-}\text{-P}$ ,  $\text{CH}_4$ ,  $\text{CO}_2$  and  $\text{N}_2\text{O}$ ) are set to zero; Scenario 2: In  
255 countries where legislative drivers are focused on water quality and losses of GHG to  
256 the atmosphere are considered less important, appropriate weighing factors are  
257 applied to  $\text{NO}_3^-$ ,  $\text{PO}_4^+$  and  $\text{NH}_4^+$ ; GHGs are not considered and are set to zero. Taking  
258 Ireland as an example, the maximum admissible concentration (MAC) for molybdate-  
259 reactive phosphorus (MRP =  $\text{PO}_4^{3-}\text{-P}$  in the current study) and  $\text{NH}_4^+$  in rivers is  $35 \mu\text{g}$   
260  $\text{P L}^{-1}$  and  $65 \mu\text{g N L}^{-1}$ , respectively, while  $\text{NO}_3^-$  in groundwater should not exceed  
261  $8.47 \text{ mg N L}^{-1}$  (the current threshold, whereas  $11.3 \text{ mg N L}^{-1}$  is the MAC). As  $\text{PO}_4^{3-}\text{-P}$   
262 is the most sensitive parameter in this case, the weighting factors for  $\text{PO}_4^{3-}\text{-P}$ ,  $\text{NH}_4^+\text{-N}$   
263 and  $\text{NO}_3\text{-N}$  are set to 1, 0.538 (35/65) and 0.004 (35/847), respectively; Scenario 3:  
264 Gaseous and water emissions are considered. Here, the weighting factor for  $\text{CO}_2$ ,  $\text{CH}_4$   
265 and  $\text{N}_2\text{O}$  is set at 1, 25 and 296, respectively, and is expressed in  $\text{CO}_2$  equivalents  
266 (IPCC, 2013). A scoring system was used across the three scenarios, with the best  
267 performing media assigned the lowest score. This methodology is very much a  
268 preliminary approach as to how a SI may be developed. However, it provides a  
269 framework to which a more nuanced holistic analysis of the performance of a  
270 bioreactor may be performed.

271

### 272 **3. Results**

273

#### 274 **3.1 Removals within each media type**

275

276 The influent and effluent  $\text{NO}_3^-\text{-N}$  concentrations in all bioreactors at the three HLRs  
277 examined are illustrated in Figure 1. For all HLRs the N removal, expressed in terms

278 of influent and effluent  $\text{NO}_3^-$ -N concentrations (single contaminant approach) in the  
279 cardboard, LPN and BBS bioreactors, were above 99.4%. The LPW and the  
280 cardboard bioreactors had comparable  $\text{NO}_3^-$ -N removals to the other bioreactors  
281 during the first and second HLRs, but both had average removals of 57.7 to 77.2% for  
282 a HLR of  $10 \text{ cm d}^{-1}$ . The ratio of C lost from the LPW bioreactors over their total  
283 period of operation (Figure 2) to the N loading on the bioreactors was, on average,  
284 22:1 – higher than the optimal ratio of around 10:1 for the occurrence of  
285 denitrification (Henze et al., 1997). This means that denitrification was not limited by  
286 C availability (bioavailability of carbon was not measured in the current study). This  
287 suggests that another process was causing the poor  $\text{NO}_3^-$ -N removal. This may have  
288 been the HRT (Figure 3), as one set of LPW bioreactors with an average HRT of 3.7 d  
289 (the lowest HRT measured in the study) had low  $\text{NO}_3^-$ -N removals. However, LPW  
290 bioreactors performed well at a HRT of 4.9 d (Figure 3). At the end of the experiment,  
291 all bioreactors were operated for 28 d at the first HLR ( $3 \text{ cm d}^{-1}$ ) to determine if the  
292 HRT limited their performance. During this time, the bioreactors returned to almost  
293 100%  $\text{NO}_3^-$ -N removal (single contaminant approach, results not shown), which  
294 confirmed that bioreactors should be operated at a HRT of between 5 and 10 d for  
295 optimal  $\text{NO}_3^-$ -N removal (assuming operational temperature, bioreactor construction  
296 and influent concentrations are similar to this study).

297

298 The bioreactors containing LPN had a large initial release of COD (up to  $5,000 \text{ mg L}^{-1}$ )  
299 <sup>1</sup>, which lasted for approximately 200 days of operation (Figure 4). During this  
300 period, up to 80% of the total carbon at each depth increment was lost from the LPN  
301 bioreactors (Figure 2). The results from all bioreactors indicate that there is a strong

302 relationship ( $R^2 = 0.73$ ) between the % of total carbon loss and cumulative COD  
303 released, according to the following equation:

304

$$305 \text{ Cumulative COD release (g)} = 5.77 \times \text{TC loss (\%)} - 3.4 \quad [3]$$

306

307 Most of the  $\text{NO}_3^-$  removal occurred within 0.4 to 0.6 m from the inlet of all  
308 bioreactors (Figure 5) for all the HLRs examined. This suggests that, excluding LPW  
309 bioreactors, there may have been some capacity to reduce the HRT without adversely  
310 affecting system performance. This is supported by Figure 3, which indicates that,  
311 with the exception of LPW bioreactors (whose performance reduced below a HRT of  
312 4.9 d),  $\text{NO}_3^-$ -N removal increased with decreasing HRT. Although there was an initial  
313 release of  $\text{NH}_4^+$ -N after system start up (Figure 6), with the exception of the LPW  
314 bioreactors, there was no significant release of  $\text{NH}_4^+$ -N at any depth increment within  
315 the bioreactors (Figure 7). This indicates that dissimilatory nitrate reduction to  
316 ammonium (DNRA), or any other microbially-mediated process, may either have  
317 only occurred at bioreactors start up when highly reducing conditions existed and  
318 when there was less dilution of the released  $\text{NH}_4^+$ -N.

319

320 Although the LPW had a P content of  $41.9 \text{ mg kg}^{-1}$  (the lowest of all the media  
321 examined; Healy et al., 2012), it had the highest concentration of  $\text{PO}_4^{3-}$ -P ( $1.1 \text{ mg}$   
322  $\text{PO}_4^{3-}$ -P  $\text{L}^{-1}$ ) in the final effluent (Figure 8). (Cardboard had a P content of  $96.1 \text{ mg kg}^{-1}$   
323 and also had a final effluent concentration close to  $1 \text{ mg PO}_4^{3-}$ -P  $\text{L}^{-1}$ ). However, in  
324 both cases, elevated P release occurred at the start of operation (at  $3 \text{ cm d}^{-1}$ ). For all  
325 media tested, the P content of the bioreactors did not change much from their initial P  
326 content (calculated per weight of soil and media mixture; results not shown). This

327 indicates that the P was relatively immobile and, even under anaerobic conditions, P  
328 was not released from the bioreactors in large amounts.

329

### 330 **3.2 Greenhouse gas emissions**

331

332 Mean daily GHG emissions associated with different media are shown in Figure 9.

333 Nitrous oxide emissions were generally extremely low, ranging from 0.04 – 8.8 mg

334  $\text{N}_2\text{O-N m}^{-2} \text{ d}^{-1}$ . With the exception of the CSO and BBS bioreactors (where emissions

335 never rose above 0.4 mg  $\text{N}_2\text{O-N m}^{-2} \text{ d}^{-1}$ ), the highest  $\text{N}_2\text{O}$  emissions occurred at the

336 highest loading rate (Figure 10), with fluxes of 1.48, 7.1 and 8.8 mg  $\text{N}_2\text{O-N m}^{-2} \text{ d}^{-1}$  for

337 cardboard, LPW and LPN, respectively. Methane emissions ranged from 0.04 mg

338  $\text{CH}_4\text{-C m}^{-2} \text{ d}^{-1}$  in the CSO bioreactors at the 10  $\text{cm d}^{-1}$  loading rate to 8.9 g  $\text{CH}_4\text{-C m}^{-2}$

339  $\text{d}^{-1}$  for cardboard at the 3  $\text{cm d}^{-1}$  loading rate. Emissions from the BBS bioreactors

340 were also high at the lowest loading rate (3.0 g  $\text{CH}_4\text{-C m}^{-2} \text{ d}^{-1}$ ). Indeed, with the

341 exception of LPW and LPN bioreactors, the highest mean daily  $\text{CH}_4\text{-C}$  emission rate

342 for all media occurred at the lowest loading rate (Figure 10). A similar emissions

343 pattern is evident for  $\text{CO}_2$ , with the highest observed flux for cardboard and BBS

344 bioreactors at the 3  $\text{cm d}^{-1}$  loading rate (5.7 g  $\text{CO}_2\text{-C m}^{-2} \text{ d}^{-1}$  and 2.25 g  $\text{CO}_2\text{-C m}^{-2} \text{ d}^{-1}$ ,

345 respectively). The  $\text{CO}_2$  rates for the CSO bioreactors were consistently the lowest for

346 all loading rates (Figure 10).

347

348 In terms of global warming potential (GWP), GHG fluxes were dominated by  $\text{CH}_4$

349 emissions (Figure 9). This is because the GWP of  $\text{CH}_4$  is 25 times higher than  $\text{CO}_2$ ,

350 even though the fluxes were similar in terms of the mass of C released. Total GHG

351 fluxes ranged from  $>0.1 \text{ g CO}_2\text{-eq m}^{-2} \text{ d}^{-1}$  for the soil control to 296 g  $\text{CO}_2\text{-eq m}^{-2} \text{ d}^{-1}$

352 for CCB at the lowest loading rate (Figure 9). Emissions from CCB varied from 85 -  
353 296 g CO<sub>2</sub>-eq m<sup>-2</sup> d<sup>-1</sup>, over 50 times higher than for all other media, with the  
354 exception of BBS at the 2 cm d<sup>-1</sup> and 5 cm d<sup>-1</sup> loading rates (Figure 9).

355

### 356 **3.3 Microbiological results**

357

358 Using one-way ANOVA, GCCs appeared to vary significantly within the bioreactors  
359 (P < 0.0001). The bacterial GCCs recorded varied significantly (P = 0.0008), with the  
360 bacterial GCCs from the cardboard bioreactors considerably greater than all other  
361 bioreactors (P<0.05). Archaeal GCCs varied significantly between the bioreactors and  
362 sampling ports (P = 0.0049; Figure 11). The abundance of the denitrifying genes *nirS*,  
363 *nirK* and *nosZ* was significantly different in all bioreactors (P = 0.0303; P = 0.0054; P  
364 = 0.0043). The most abundant denitrifying gene was *nirS*, for which the highest GCCs  
365 were recorded 0.2 m from the inlet of the cardboard bioreactor (1.32 x 10<sup>8</sup> GCC g<sup>-1</sup>  
366 dry substrate). *NirS* GCCs from the cardboard bioreactors were significantly greater  
367 than the CSO bioreactors (P<0.05). Overall, recorded *nirS* GCCs were greater than  
368 *nirK* GCCs. The *nirK* GCCs in the cardboard bioreactors were significantly higher  
369 than the CSO, LPN and LPW bioreactors (P<0.05; P<0.05; P<0.05). The *nosZ* GCCs  
370 in the cardboard bioreactors were also significantly greater than the CSO, BBS and  
371 LPN bioreactors (P<0.01; P<0.05; P<0.05). Using Primer v6, a Bray-Curtis  
372 resemblance matrix was generated for each bioreactor and sampling port using square  
373 root transformed mean 16S rRNA, *nirS*, *nirK* and *nosZ* gene copy abundances. The  
374 resultant resemblance matrices from the Bray-Curtis analysis of the total and  
375 denitrifying bacterial communities (from molecular data) showed that there was  
376 clustering between sampling ports from each bioreactor i.e. CSO bioreactors display a

377 90-100% similarity between its sampling ports (results not shown). The LPN and  
378 LPW bioreactor sampling ports were clustered together and had an 80-90% similarity,  
379 whereas the CSO and cardboard bioreactors displayed a 60-70% similarity.

380

## 381 **4. Discussion**

382

### 383 **4.1 Nitrate removal**

384

385 The maximum  $\text{NO}_3^-$ -N removal rate measured was approximately  $3.5 \text{ g NO}_3^- \text{-N m}^{-3} \text{ d}^{-1}$ ,  
386 which is similar to other laboratory studies using wood-based media (e.g., 1.3 to 6.2  
387  $\text{g NO}_3^- \text{-N m}^{-3} \text{ d}^{-1}$ , Warneke *et al.*, 2011b; 3.9  $\text{g NO}_3^- \text{-N m}^{-3} \text{ d}^{-1}$ , Grennan *et al.*, 2009;  
388 3.4  $\text{g NO}_3^- \text{-N m}^{-3} \text{ d}^{-1}$ , Schmidt and Clark, 2012), but much lower than some studies  
389 using wood-based media (e.g., Robertson, 2010). Although the total carbon content  
390 and the ratio of C lost from the bioreactors over their total period of operation to the  
391 N loading on the bioreactors was adequate to sustain denitrification, the  
392 bioavailability of C was not measured. Other methods may be used to assess the  
393 denitrification potential of bioreactor media, such as Schmidt and Clark (2013), who  
394 assessed the long-term denitrification potential of various media by calculating the  
395 effluent DOC load (in  $\text{g DOC m}^{-3}$  of media per day) over time. It is unlikely that  $\text{NO}_3^-$   
396 -N removal rates were limited by the influent  $\text{NO}_3^-$ -N concentration, which was  
397 between 19.5 and 32.5  $\text{mg L}^{-1}$ , or by the slow reaction kinetics in the conversion of  
398  $\text{NO}_3^-$  to  $\text{N}_2$ , as  $\text{NO}_3^-$ -N removals increased with reducing HRT. However, bioreactor  
399 performance may have been affected by the operational temperature ( $10^\circ\text{C}$ ), as shown  
400 in other studies (Cameron and Schipper, 2010; Warneke *et al.*, 2011b).

401

402 Nitrite reductase genes (*nirS* and *nirK*) ranged from  $10^4$  to  $10^7$  GCC  $g^{-1}$  dry substrate  
403 in this study (Figure 11), which is in the same range measured by Warneke *et al.*  
404 (2011b). As the  $NH_4^+$ -N concentration at the outlet from all bioreactors was generally  
405 low, it is unlikely that DNRA contributed significantly to  $NO_3^-$ -N removal. This  
406 indicates that denitrification was most likely the main mechanism for  $NO_3^-$ -N  
407 removal, the extent of which was affected by the bioreactor HRT (Figure 3). The pH  
408 measured along the sampling ports and the outlet was in the optimal range for  
409 denitrifiers (pH 7–8; Tchobanoglous *et al.*, 2003). The inverse relationship between  
410 the HRT and  $NO_3^-$ -N removal rate, combined with the lack of a discernible trend in  
411 nitrite reductase genes along the bioreactors (Figure 11), suggests that, with the  
412 exception of LPW bioreactors, a shorter HRT would not have any adverse impact on  
413 performance. These findings are, however, very specific to this study. In field-scale  
414 bioreactors, HLR is very difficult to control, so bioreactors should be designed so that  
415 they have an adequate HRT for the effective reduction of  $NO_3^-$ .

416

#### 417 **4.2 Denitrifying bacterial communities**

418

419 The CCB bioreactors had the greatest average abundance of denitrification genes but  
420 lowest number of denitrification genes as a proportion of total bacteria and the highest  
421 number of 16S rRNA GCC  $g^{-1}$ . Excluding the control bioreactors, the other  
422 bioreactors (BBS, LPN and LPW) had a similar number of denitrification genes and  
423 total bacterial DNA, and both parameters were at least an order of magnitude less than  
424 the cardboard bioreactors. The LPN and LPW bioreactors had the highest number of  
425 denitrification genes as a proportion of total bacteria. This implies that a greater  
426 proportion of C in cardboard bioreactors was consumed by non-denitrifying bacteria,

427 fungi or yeasts, whereas a greater proportion of C in the LPN and LPW bioreactors  
428 was consumed by denitrifiers. In order to verify this, further work would be necessary  
429 targeting alternative stains. The fact that a greater proportion of denitrifiers were  
430 present in the LPN/LPW media coincided with higher N<sub>2</sub>O emissions, which were  
431 observed in both media at the highest loading rate. This increase in N<sub>2</sub>O level also  
432 coincided with a decrease in the efficiency of NO<sub>3</sub><sup>-</sup> removal at the highest loading  
433 rate. It may indicate either partial denitrification to N<sub>2</sub>O *in situ* or degassing of  
434 dissolved N<sub>2</sub>O in the original water in the column.

435

436 The ratio of *nirS/nirK* and total number of nitrite reductase genes ( $\Sigma nir$ )/*nosZ* was  
437 similar between replicate bioreactors and within each 0.2-m-depth in every bioreactor.  
438 There was no indication that populations of denitrifying or non-denitrifying bacteria  
439 were grouped at any particular point within the bioreactors (i.e. towards the inlet or  
440 outlet). The nutrient concentrations measured at each 0.2-m-depth increment were  
441 consistent with this finding (Figures 5 and 7). There appears to be a greater variation  
442 in denitrifying gene number and presence between the reactors than within an  
443 individual reactor, based on the sampling resolution used. Indicating microbial  
444 populations and activity established in each bioreactor therefore reflect and respond to  
445 the nature of the media therein (and microbial evolution of the system), as opposed to  
446 operation of the bioreactor (i.e. HRT). Overall, this suggests that gene analysis may  
447 be employed to reliably assess the relative dominance of the denitrifying microbial  
448 populations. Further work is necessary to determine if it could be used as a potential  
449 proxy for bioreactor design and optimisation.

450

451 **4.3 Greenhouse gases**

452

453 Anoxic to anaerobic conditions in the bioreactors resulted in high levels of CH<sub>4</sub> efflux  
454 and relatively low CO<sub>2</sub> and N<sub>2</sub>O loss. Anaerobic conditions result in the complete  
455 denitrification of nitrite and subsequently nitrate to N<sub>2</sub>. As a result, the N<sub>2</sub>O flux in the  
456 bioreactors was very low and negative fluxes were observed in some cases; in these  
457 instances, *nir* GCCs were lower than *nosZ* GCCs. A significant flux was only  
458 observed at higher HLRs, where the presence of dissolved O<sub>2</sub> in the influent may  
459 allow some partial denitrification to N<sub>2</sub>O. This, combined with the higher pressures in  
460 the system, may subsequently result in the degassing of dissolved N<sub>2</sub>O, and coincided  
461 with decreased nitrate removal from the bioreactors.

462

463 Apart from the cardboard medium, CO<sub>2</sub> release from heterotrophic respiration was  
464 very low compared with normal rates of (7- 30 g CO<sub>2</sub> m<sup>-2</sup> d<sup>-1</sup>) of soil respiration  
465 (Lloyd and Taylor, 1994). The higher rate of CO<sub>2</sub> and CH<sub>4</sub> efflux in the cardboard  
466 bioreactors reflected the successional mobilisation of organic C *via* heterotrophic and  
467 anaerobic respiration, and was also related to the archaeal 16SrRNA GCC abundance.  
468 Carbon within the media was utilised principally by denitrifying bacteria, generating  
469 CO<sub>2</sub> that was either directly emitted or consumed by methanogens as the terminal  
470 electron acceptor in methanogenesis (Wolin and Miller, 1987). The lower rates  
471 observed in LPW, LPN and CSO bioreactors (0.02 mg CH<sub>4</sub> m<sup>-2</sup> d<sup>-1</sup> to 0.34 mg CH<sub>4</sub> m<sup>-2</sup>  
472 d<sup>-1</sup> for soil and LPW bioreactors, respectively) were comparable to typical values of  
473 diffusional (non-ebullition) methane fluxes from peatlands, which range from 1.5–480  
474 mg CH<sub>4</sub> m<sup>-2</sup> d<sup>-1</sup> (Coulthard *et al.*, 2009). The higher rates in the cardboard (8.8 mg  
475 CH<sub>4</sub> m<sup>-2</sup> d<sup>-1</sup>) and, to a lesser extent, BBS bioreactors (3 mg CH<sub>4</sub> m<sup>-2</sup> d<sup>-1</sup>), reflect higher  
476 rates of microbial activity presumably due to more labile C sources. Emissions from

477 both these media were greatest at the lowest loading rates (2.5 to 8.8 g CH<sub>4</sub>-C m<sup>-2</sup> d<sup>-1</sup>),  
478 equating to an annual methane loss of between 1.3 and 4.3 kg CH<sub>4</sub> m<sup>-2</sup> yr<sup>-1</sup>. These  
479 emissions are similar to localised methane ebullition from peatlands, where fluxes can  
480 range from 1.2 to 26 g CH<sub>4</sub>-C m<sup>-2</sup> d<sup>-1</sup> (Glazer *et al.*, 2004; Tokida *et al.*, 2007).

481

482 The high total GHG emissions from CCB and BBS bioreactors were dominated by  
483 methane and were 50 times higher than other media, which had comparable or better  
484 nitrate removal. As such, these media should be avoided in bioreactors or if they are  
485 used, some form of remedial action, such as soil capping, should be utilised to oxidise  
486 some of the methane and reduce this flux to the atmosphere (Stern *et al.*, 2007).

487

#### 488 **4.4 Identification of optimum loading rates considering pollution swapping**

489

490 The net flux of each parameter of interest in this study is shown in Table 3 and the SI  
491 calculations for three scenarios (1=only NO<sub>3</sub><sup>-</sup> considered; 2=all mixed contaminants  
492 in water; and 3=water and gaseous emissions) are presented in Table 4. For Scenario  
493 1, LPW bioreactors performed best at the lowest HLR, and cardboard and LPN  
494 bioreactors performed best at the two higher HLRs. In Scenario 2, BBS bioreactors  
495 had the best performance across all HLRs. In Scenario 3, LPN bioreactors performed  
496 best at HLRs of 3 and 5 cm d<sup>-1</sup>, whereas LPW bioreactors performed best at a HLR of  
497 10 cm d<sup>-1</sup>. Considering all water quality and gaseous parameters for the three  
498 scenarios, analysed at each HLR, the LPN bioreactors performed best. However, there  
499 was an 80% reduction in TC from the LPN bioreactors over its operation period  
500 (approximately 560 days) (Figure 2). In comparison, the LPW bioreactors only

501 experienced a TC loss of approximately 27% over 745 days of operation, which  
502 suggests this type of bioreactor may have greater longevity than LPN bioreactors.

503

504 It is important for research to start moving from single contaminant to mixed  
505 contaminant mitigation, as conceptualised by Fenton *et al.* (2014). The type of  
506 analysis conducted in this study is considerably simplified, but highlights the huge  
507 disadvantages of the single contaminant approach. In reality, attributing weighting  
508 factors to both dissolved contaminants and GHGs would be considerably more  
509 complex, and require consideration of their respective costs and benefits, local  
510 legislation and environmental conditions, as well as cognisance of the fact that  
511 legislation will change over time. If total removal of mixed contaminants, apart from  
512 achievement of maximum admissible concentrations or targets, is the goal, more  
513 efficient systems will need to be envisaged for the future. The co-location of  
514 denitrifying bioreactor and adsorption structures in sequence – termed “permeable  
515 reactive interceptors” – is a move in this direction (Fenton *et al.*, 2014).

516

## 517 **5. Conclusions**

518

519 The way in which the performance of denitrifying bioreactors is assessed can lead to  
520 different conclusions about optimum HRT and media selection. When  $\text{NO}_3^-$  removal  
521 only was assessed (single contaminant approach), there was a net removal in all  
522 bioreactors, which increased as HRT reduced. All bioreactors performed best at HRTs  
523 of around 5 days. When all contaminants ( $\text{NO}_3^-$ ,  $\text{NH}_4^+$  and  $\text{PO}_4^{3-}$ ) were considered,  
524 there was a net flux of contaminants from all columns, which further increased when  
525 greenhouse gas emissions were also considered. To reduce pollution swapping from

526 bioreactors, suitable media could be placed in sequence in the filters, which would be  
527 capable of reducing the contaminant of interest before final discharge. Based on the  
528 study results, LPN bioreactors appeared to be the most effective design, across all  
529 HRTs and scenarios, at effectively treating  $\text{NO}_3^-$ , while limiting pollution swapping.  
530 However, a substantial amount of carbon was lost over a relatively short period  
531 (around 80% of the initial content of the LPN bioreactors). This indicates that a more  
532 commonly available filter media, such as LPW, may be more suitable for the long-  
533 term operation of bioreactors.

534

535 Microbiological testing of the filter media at the end of the experiment indicated that  
536 denitrification was most likely the main mechanism for  $\text{NO}_3^-$ -N removal and that  
537 there was no clustering of the denitrifying or non-denitrifying bacteria at any  
538 particular point within the bioreactors. The addition of carbon appeared to affect the  
539 abundance of denitrifiers possessing the targeted functional genes. Moreover, the  
540 cardboard bioreactor contained the highest abundance of denitrifying microorganisms  
541 compared with the other bioreactors, indicating that the source of carbon influenced  
542 the abundance of denitrifying microbes. Microbiological analyses, such as those  
543 performed in this study, could be used as a proxy for system performance at various  
544 HRTs with further testing. However, this analysis could not be performed in the  
545 current study, as the microbiological testing was conducted in the columns having  
546 been subjected to three HLRs.

547

548 **Acknowledgements**

549

550 This study was funded under the Department of Agriculture, Fisheries and Food under  
551 the Research Stimulus Programme 2007 (RSF 07 525).

552

553

554

555

556

557

558

559

560

561

562

563

564

565

566

567

568

569

570

571

572

573

574

575 **References**

576

577 APHA, 1995. Standard methods for examination of water and wastewater, 19<sup>th</sup> ed.

578 American Public Health Association, Washington, DC.

579

580 Barrett, M., Jahangir, M.M.R., Lee, C., Smith, C.J., Bhreathnach, N., Collins, G.,

581 Richards, K.G., O’Flaherty, V., 2013. Abundance of denitrification genes under

582 different piezometer depths in four agricultural groundwater sites. *Environmental*

583 *Science and Pollution Research* 20 (9), 6646-6657.

584

585 Braker, G., Fesefeldt, A., Witzel K.P., 1998. Development of PCR primer systems for

586 amplification of nitrite reductase genes (*nirK* and *nirS*) to detect denitrifying bacteria

587 in environmental samples. *Applied and Environmental Microbiology* 64 (10), 3769-

588 3775.

589

590 Cameron, S.G., Schipper, L.A., 2010. Nitrate removal and hydraulic performance of

591 organic carbon for use in denitrification beds. *Ecological Engineering* 36 (11), 1588 –

592 1595.

593

594 Christianson, L.E., Bhandari, A., Helmers, M.J., 2011. Pilot-scale evaluation of

595 denitrification drainage bioreactors: reactor geometry and performance. *ASCE*

596 *Journal of Environmental Engineering* 137 (4), 213 – 220.

597

598 Chun, J.A., Cooke, R.A., Eheart, J.W., Kang, M.S., 2009. Estimation of flow and

599 transport parameters for woodchip-based bioreactors: I. laboratory-scale bioreactor.

600 *Biosystems Engineering* 104 (3), 384 – 395.

601

602 Clarke, K.R, Somerfield, P.J., Chapman, M.G., 2006. On resemblance measures for

603 ecological studies, including taxonomic dissimilarities and a zero-adjusted Bray–

604 Curtis coefficient for denuded assemblages. *Journal of Experimental Marine Biology*

605 *and Ecology* 330 (1), 55–80.

606

607 Coulthard, T.J., Baird, A. J., Ramirez, J., Waddington J. M., 2009. Methane dynamics

608 in peat: importance of shallow peats and a novel reduced-complexity

609 approach for modeling ebullition. In: A.J. Baird, L.R. Belyea, X. Comas, A. S. Reeve,

610 and L. D. Slater (Eds.) *Carbon Cycling in Northern Peatlands*. American Geophysical

611 Union, Washington.

612

613 Durand, P., Breuer, L., Johnes, P.J., 2011. Nitrogen processes in aquatic ecosystems.

614 Pp. 126-146. In: M.A. Sutton, C.M. Howard, J.W. Erisman, G. Billen, A. Bleeker, P.

615 Grennfelt, H. van Grinsven, B. Grizzetti (eds.), *The European Nitrogen Assessment-*

616 *Sources, Effects and Policy Perspectives*. Cambridge University Press, Cambridge.

617

618 Elgood, Z., Robertson, W.D., Schiff, S.L., Elgood, R., 2010. Nitrate removal and

619 greenhouse gas production in a stream-bed denitrifying bioreactor. *Ecological*

620 *Engineering* 36 (11), 1575 – 1580.

621

622 Fenton, O., Richards, K.G., Kirwan, L., Healy, M.G., 2009. Factors affecting nitrate

623 distribution in shallow groundwater using a beef farm in south eastern Ireland. *Journal*

624 *of Environmental Management* 90 (10), 3135 – 3146.

625  
626 Fenton, O., Schulte, R.P.O., Jordan, P., Lalor, S., Richards, K.G., 2011. Time lag: a  
627 methodology for the estimation of vertical and horizontal travel and flushing  
628 timescales to nitrate threshold concentrations in Irish aquifers. *Environmental Science*  
629 *and Policy* 14 (4), 419-431.  
630  
631 Fenton, O., Healy, M.G., Brennan, F., Jahangir, M.M.R., Lanigan, G.J., Richards,  
632 K.G., Thornton, S.F., Ibrahim, T.G., 2014. Permeable reactive interceptors – blocking  
633 diffuse nutrient greenhouse gases losses in key areas of the farming landscape.  
634 *Journal of Agricultural Science*. In press. doi:10.1017/S0021859613000944  
635  
636 Flechard C.R., Nemitz E., Smith R.I., Fowler D., Vermeulen A.T., Bleeker A., Erisman  
637 J.W., Simpson D., Zhang L., Tang Y.S., and Sutton M.A., 2011. Dry deposition of  
638 reactive nitrogen to European ecosystems: a comparison of inferential models across the  
639 NitroEurope network. *Atmospheric Chemistry and Physics* 11 (6), 2703–2728.  
640  
641 Fujinuma, R., Venterea, R.T., Ranaivoson, A., Moncrief, J., Dittrich, M. 2011. On-  
642 site wood-chip bioreactors could reduce indirect nitrous oxide emissions from tile  
643 drain waters. In: *Proceedings of Nutrient Efficiency and Management Conference*.  
644 MN Department of Agriculture, Minnesota, February 2011.  
645  
646 Glaser, P.H., Chanton, J.P., Morin, P., Rosenberry, D.O., Siegel, D.I., Ruud, O.,  
647 Chasar, L.I., Reeve, A.S., 2004. Surface deformations as indicators of deep ebullition  
648 fluxes in a large northern peatland, *Global Biogeochemical Cycles* 18 (1), 1 – 15.  
649  
650 Grennan, C.M., Moorman, T.B., Parkin, T.B., Kaspar, T.C., Jaynes, D.B., 2009.  
651 Denitrification in wood chip bioreactors at different water flows. *Journal of*  
652 *Environmental Quality* 38 (4), 1664 – 1671.  
653  
654 Grizzetti, B., Bouraoui, F., Aloe, A., 2012. Changes in nitrogen and phosphorus loads  
655 to European seas. *Global Change Biology* 18 (2), 769-782.  
656  
657 Healy, M.G., Rodgers, M., Mulqueen, J., 2006. Denitrification of a nitrate-rich  
658 synthetic wastewater using various wood-based media materials. *Journal of*  
659 *Environmental Science and Health, Part A* 41 (5), 779 – 788.  
660  
661 Healy, M.G., Ibrahim, T.G., Lanigan, G.J., Serrenho, A.J., Fenton, O., 2012. Nitrate  
662 removal rate, efficiency and pollution swapping potential of different organic carbon  
663 media in laboratory denitrification bioreactors. *Ecological Engineering* 40 (March  
664 2012), 198 – 209.  
665  
666 Henry, S., Bru, D., Stes, B., Hallet, S., Philippot, L., 2006. Quantitative detection of  
667 the *nosZ* gene, encoding nitrous oxiden reductase, and comparison of the abundances  
668 of 16S rRNA, *narG*, *nirK*, and *nosZ* genes in soils. *Applied and Environmental*  
669 *Microbiology* 72 (8), 5181–5189.  
670  
671 Henze, M., Harremoës, P., Jansen, J.L.C., Arvin, E., 1997. *Wastewater treatment:*  
672 *biological and chemical processes*. Springer, Berlin.  
673

674 Hutchinson, G.L., Mosier, A.R., 1981. Improved soil cover method for field  
675 measurement of nitrous oxide fluxes. *Soil Science Society of America Journal* 45 (2),  
676 311 – 316.  
677  
678 IPCC, 2013. *Climate change 2013: The physical science basis. Contribution of*  
679 *Working Group I to the fifth assessment report of the intergovernmental panel on*  
680 *climate change, Ch.8, p. 714.*  
681  
682  
683 Kandeler, E., Deiglmayr, K., Tscherko, D., Bru, D., Philippot, L., 2006. Abundance of  
684 *narG*, *nirS*, *nirK*, and *nosZ* Genes of denitrifying bacteria during primary successions  
685 of a glacier foreland. *Applied and Environmental Microbiology* 72 (9), 5957–5962.  
686  
687 Lee, C., Kima, J., Hwang, K., O’Flaherty, V., Hwang, S., 2009. Quantitative  
688 analysis of methanogenic community dynamics in three anaerobic batch digesters  
689 treating different wastewaters. *Water Research* 43 (1), 157-165.  
690  
691 Levenspiel, O. 1999. *Chemical reaction engineering.* John Wiley and Sons, New  
692 York.  
693  
694 Lloyd J., Taylor J.A., 1994. On the temperature dependence of soil respiration.  
695 *Functional Ecology* 8, 315-323.  
696  
697 Moorman, T.B., Parkin, T.B., Kaspar, T.C., Jaynes, D.B., 2010. Denitrification  
698 activity, wood loss, and N<sub>2</sub>O emissions over 9 years from a wood chip bioreactor.  
699 *Ecological Engineering* 36 (11), 1567 – 1574.  
700  
701 Richardson, D., Felgate, H., Watmough, N., Thomson, A., Baggs, E., 2009.  
702 Mitigating release of the potent greenhouse gas N<sub>2</sub>O from the nitrogen cycle – could  
703 enzymic regulation hold the key? *Trends in Biotechnology* 27 (7), 388 – 397.  
704  
705 Rivett, M.O., Buss, S.R., Morgan, P., Smith, J.W., Bemment, C.D., 2008. Nitrate  
706 attenuation in groundwater: a review of biogeochemical controlling processes. *Water*  
707 *Research* 42 (16), 4215 – 4232.  
708  
709 Robertson, W.D., 2010. Nitrate removal rates in woodchip media of varying age.  
710 *Ecological Engineering* 36 (11), 1581 – 1587.  
711  
712 Schipper, L.A., Robertson, W.D., Gold, A.J., Jaynes, D.B., Cameron, S.C., 2010.  
713 Denitrifying bioreactors – an approach to reducing nitrate loads to receiving waters.  
714 *Ecological Engineering* 36 (11), 1532-1543.  
715  
716 Schmidt, C.A., Clark, M.W., 2012. Efficacy of a denitrification wall to treat  
717 continuously high nitrate loads. *Ecological Engineering* 42 (May 2012), 203 – 211.  
718  
719 Stern, J.C., Chanton, J., Abichou, T., Powelson, D., Yuan, L., Escoriza, S., Bogner, J.,  
720 2007. Use of a biologically active cover to reduce landfill methane emissions and  
721 enhance methane oxidation. *Waste Management* 27 (9), 1248-1258.  
722

723 Tchobanoglous, G., Burton, F.L., Stensel, H.D., 2003. Wastewater engineering,  
724 Treatment and Reuse. McGraw Hill, New York, NY.  
725

726 Tokida, T., Miyazaki, T., Mizoguchi, M., Nagata, O., Takakai, F., Kagemoto, A.,  
727 Hatano, R., 2007. Falling atmospheric pressure as a trigger for methane ebullition  
728 from a peatland, *Global Biogeochemical Cycles* 21, GB2003  
729

730 Yu, Y., Lee, C., Kim, J., Hwang, S., 2005. Group-specific primer and probe sets to  
731 detect methanogenic communities using quantitative real-time polymerase chain  
732 reaction. *Biotechnology and Bioengineering* 89 (6), 670–679.  
733

734 Warneke, S., Schipper, L.A., Bruesewitz, D.A., McDonald, I., Cameron, S., 2011a.  
735 Rates, controls and potential adverse effects of nitrate removal in a denitrification bed.  
736 *Ecological Engineering* 37 (3), 511-522.  
737

738 Warneke, S., Schipper, L.A., Matiasek, M.G., Scow, K.M., Cameron, S., Bruesewitz,  
739 D.A., McDonald, I.R., 2011b. Nitrate removal, communities of denitrifiers and  
740 adverse effects in different carbon substrates for use in denitrification beds. *Water*  
741 *Research* 45 (17), 5463 – 5475.  
742

743 Wolin, M.J., Miller, T.L., 1987. Bioconversion of organic carbon to CH<sub>4</sub> and CO<sub>2</sub>.  
744 *Geomicrobiology* 5 (3-4), 239-59.  
745

746 Xu, Z., Shao, L., Yin, H., Chu, H., Yao, Y., 2009. Biological denitrification using  
747 corn cobs as a carbon source and biofilm carrier. *Water Environment Research* 81 (3),  
748 242-247.  
749  
750  
751  
752  
753  
754  
755  
756  
757

758  
759  
760  
761  
762

763 **Table 1.** Media used in denitrification bioreactors, period of operation (d), hydraulic retention time (HRT; d), nitrate (NO<sub>3</sub><sup>-</sup>-N) removal  
 764 (expressed as difference between inlet and outlet concentration; %) at each hydraulic loading rate (3, 5 and 10 cm d<sup>-1</sup>) applied to the bioreactors.  
 765

Media <sup>a</sup>	Column	HLR (cm d <sup>-1</sup> )			HLR (cm d <sup>-1</sup> )			HLR (cm d <sup>-1</sup> ) <sup>b</sup>		
		3	5	10	3	5	10	3	5	10
		Period of operation (d)			HRT (d)			NO <sub>3</sub> -N removal		
LPW	1	460	238	47	17.4	7.7	4.9	99.6	82.6	58.8
	2				13.0	8.1	3.7	99.6	93.1	57.7
	3				14.8	9.2	5.7	99.7	99.4	77.2
Cardboard	1	438	237	47	10.2	6.7	4.0	99.7	99.5	99.7
	2				8.5	7.4	4.8	99.5	99.4	99.7
	3				10.9	6.9	3.5	99.8	99.4	99.7
LPN	1	278	237	47	9.9	9.6	4	99.8	99.4	99.7
	2				11.6	6.7	4	99.7	99.2	99.7
	3				9.9	9.5	3.6	99.9	99.4	99.7
BBS	1	231	133	47	13.9	7.0	3.5	-	99.4	99.7
	2				21.7	8.8	3.9	-	99.7	99.7
	3				18.2	7.3	3.6	-	99.5	99.7
Soil	1	257	134	47	15.5	6.1	4.6	16.5	4.6	-1.4
	2				11.8	6.4	3.8	28.0	0.9	-0.4

766 <sup>a</sup> LPW = lodgepole pine woodchips; LPN = lodgepole pine needles; BBS = barley straw

767 <sup>b</sup> Nitrate removal and efficiency reported at steady-state only. Steady-state was not attained at a HLR of 3 cm d<sup>-1</sup> for BBS (Healy et al., 2012).

768  
 769  
 770  
 771  
 772  
 773  
 774

775 **Table 2** Realtime primer and probes for microbial analysis (adapted from Barrett et al., 2013)

Gene	Standard strains	Oligoneucleotide <sup>c</sup>	Sequences (5' – 3')	Amplicon size (bp)	Reference
<i>nirS</i>	<i>Pseudomonas Stutzeri</i> ATCC 14405 <sup>a</sup>	F: <i>nir</i> SCd3aF R: <i>nir</i> SR3cd	AACGYSAAGGARACSGG GASTTCGGRTGSGTCTTSAYGAA	425	Kandeler et al. (2006)
<i>nirK</i>	<i>Alcalignes</i> Species DSMZ 30128 <sup>b</sup>	F: <i>nir</i> k 1F R: <i>nir</i> k 5R	GG(A/C) ATG GT (G/T) CC(C/G) TGG CA GCC TCG ATC AG (A/G) TT(A/G) TGG	514	Braker et al. (1998)
<i>nosZ</i>	<i>Bradyrhizobium</i> <i>Japonicum</i> USDA 110 <sup>c</sup>	F: <i>nosz</i> 2 F R: <i>nosz</i> 2 R	CG(C/T)TGTT(C/A/C)TCGACAGCCAG CAKRTGCAKSGCRTGGCAGAA	267	Henry et al. (2006)
Bacterial 16SrRNA	<i>Escherichia coli</i> K12 <sup>d</sup>	F: BAC 338F R: BAC 805R P: BAC516F	ACTCCTACGG GAGGCAG GACTACCAGGGTATCTAATCC TGC CAG CAG CCG CGG TAA TAC	466	Yu et al. (2005)
Archaeal 16SrRNA		F:ARC787 R:ARC1059 P:ARC915	ATTAG ATACC CSBGT AGTCC AGGAA TTGGC GGGGG AGCAC GCCAT GCACC WCCTC T	273	Yu et al. (2005)

776 <sup>a</sup> ATCC, American type culture collection <sup>b</sup> DSMZ, The German Resource Centre for Biological Material <sup>c</sup> USDA, United States Department of Agriculture <sup>d</sup> Gift <sup>e</sup> P, TaqMan probe; F,  
777 Forward primer; R, Reverse primer  
778

779

780

781

782

783

784

785

786

787 **Table 3.** Net fluxes (in  $\text{g m}^{-2} \text{d}^{-1}$ )  $\pm$  standard deviations (in brackets) of major dissolved compounds and greenhouse gases (expressed as  $\text{CO}_2$  equivalents per unit surface area  
788 per day.) from laboratory scale denitrifying bioreactors, operated at steady-state, for the three hydraulic loading rates (HLRs), 3, 5 and  $10 \text{ cm d}^{-1}$ . Negative and positive fluxes  
789 indicate remediation and production of the compound, respectively.

HLR ( $\text{cm d}^{-1}$ )	Media <sup>a</sup>	$\text{NO}_3^- \text{-N}$	$\text{NH}_4^+ \text{-N}$	$\text{PO}_4^{3-} \text{-P}$	$\text{CH}_4$	$\text{CO}_2$	$\text{N}_2\text{O}$
3	LPW	-0.81 (0)	0.11 (0.01)	0.003 (0)	4.01 (2.04)	3.86 (1.04)	0.57 (0.39)
	Cardboard	-0.60 (0)	0.05 (0.01)	0.001 (0)	296.03 (26.67)	21.04 (4.41)	0.04 (0.03)
	LPN	-0.78 (0)	0.05 (0.02)	0.000 (0)	2.52 (1.26)	5.13 (1.85)	0.10 (0.04)
	BBS	-0.75 (0)	0.03 (0.01)	0.001 (0)	100.29 (55.69)	8.26 (1.35)	0.22 (0.08)
5	LPW	-1.00 (0.1)	0.03 (0)	0.018 (0.013)	11.57 (2.29)	1.51 (0.37)	1.48 (1.09)
	Cardboard	-1.09 (0)	0.03 (0.02)	0.001 (0)	99.43 (35.48)	6.88 (3.73)	0.02 (0.04)
	LPN	-1.08 (0)	0.03 (0)	0.002 (0)	0.70 (0.55)	1.38 (0.57)	0.09 (0.70)
	BBS	-1.08 (0)	0.02 (0)	0.001 (0)	38.04 (18.57)	3.10 (0.50)	0.13 (0.09)
10	LPW	-1.46 (0.24)	0.07 (0.03)	0.003 (0.001)	0 (0.01)	1.47 (0.34)	3.29 (2.88)
	Cardboard	-2.15 (0)	0.05 (0.03)	0.002 (0)	85.36 (23.19)	6.12 (2.33)	0.69 (0.78)
	LPN	-2.19 (0)	0.06 (0.01)	0.003 (0.002)	3.71 (1.47)	1.66 (0.65)	4.11 (3.28)
	BBS	-2.12 (0)	0.03 (0)	0 (0)	4.28 (1.84)	1.42 (0.69)	0.02 (0.12)

790 <sup>a</sup> LPW = lodgepole pine woodchips; LPN = lodgewood pine needles; BBS = barley straw

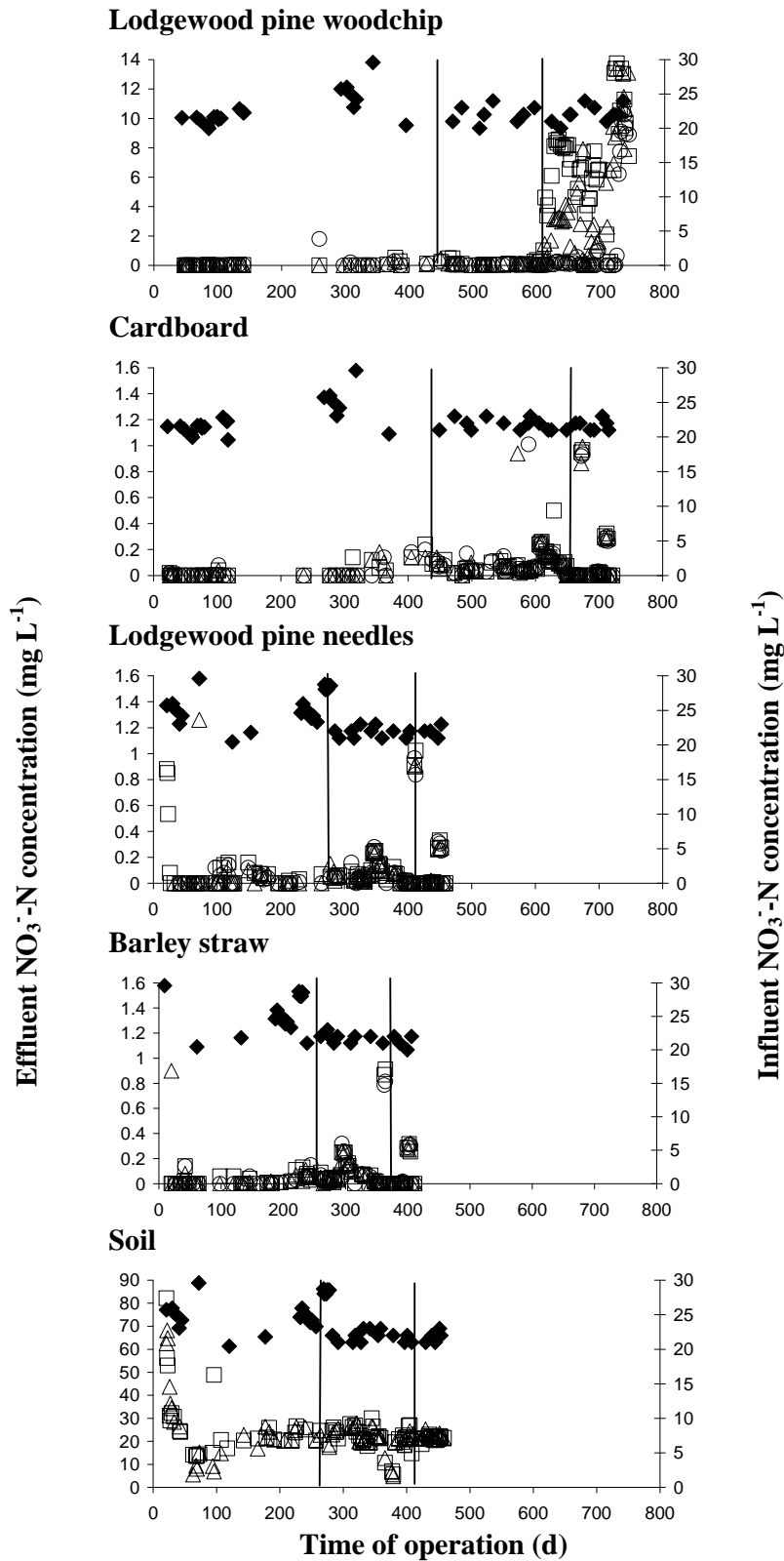
791 **Table 4.** Net flux ( $\text{g m}^{-2} \text{d}^{-1}$ ) and sustainability index (SI) calculations, calculated  
 792 from Table 3, for the filter media for three scenarios (see text for explanation).  
 793 Negative and positive net fluxes indicate removal and production of the compound,  
 794 respectively. A high SI indicates poor performance, a low SI indicates good  
 795 performance.  
 796

HLR	Media <sup>a</sup>	Scenario 1		Scenario 2		Scenario 3		Overall ranking <sup>b</sup>
( $\text{cm d}^{-1}$ )		Net flux ( $\text{g m}^{-2} \text{d}^{-1}$ )	SI	Net flux ( $\text{g m}^{-2} \text{d}^{-1}$ )	SI	Net flux ( $\text{g m}^{-2} \text{d}^{-1}$ )	SI	
3	LPW	-0.81	1	0.06	3	7.74	2	7
	Cardboard	-0.60	4	0.03	4	316.56	4	11
	LPN	-0.78	2	0.02	1	7.02	1	5
	BBS	-0.75	3	0.01	2	108.05	3	7
5	LPW	-1.00	3	0.03	3	13.61	2	7
	Cardboard	-1.09	1	0.01	1	105.27	4	6
	LPN	-1.08	2	0.01	2	1.12	1	4
	BBS	-1.08	2	0.01	1	40.21	3	6
10	LPW	-1.46	4	0.03	4	3.37	1	8
	Cardboard	-2.15	2	0.02	2	90.07	4	8
	LPN	-2.19	1	0.03	1	7.35	3	7
	BBS	-2.12	3	0.01	3	3.63	2	6

797 <sup>a</sup> LPW = lodgewood pine woodchips; LPN = lodgewood pine needles; BBS = barley straw

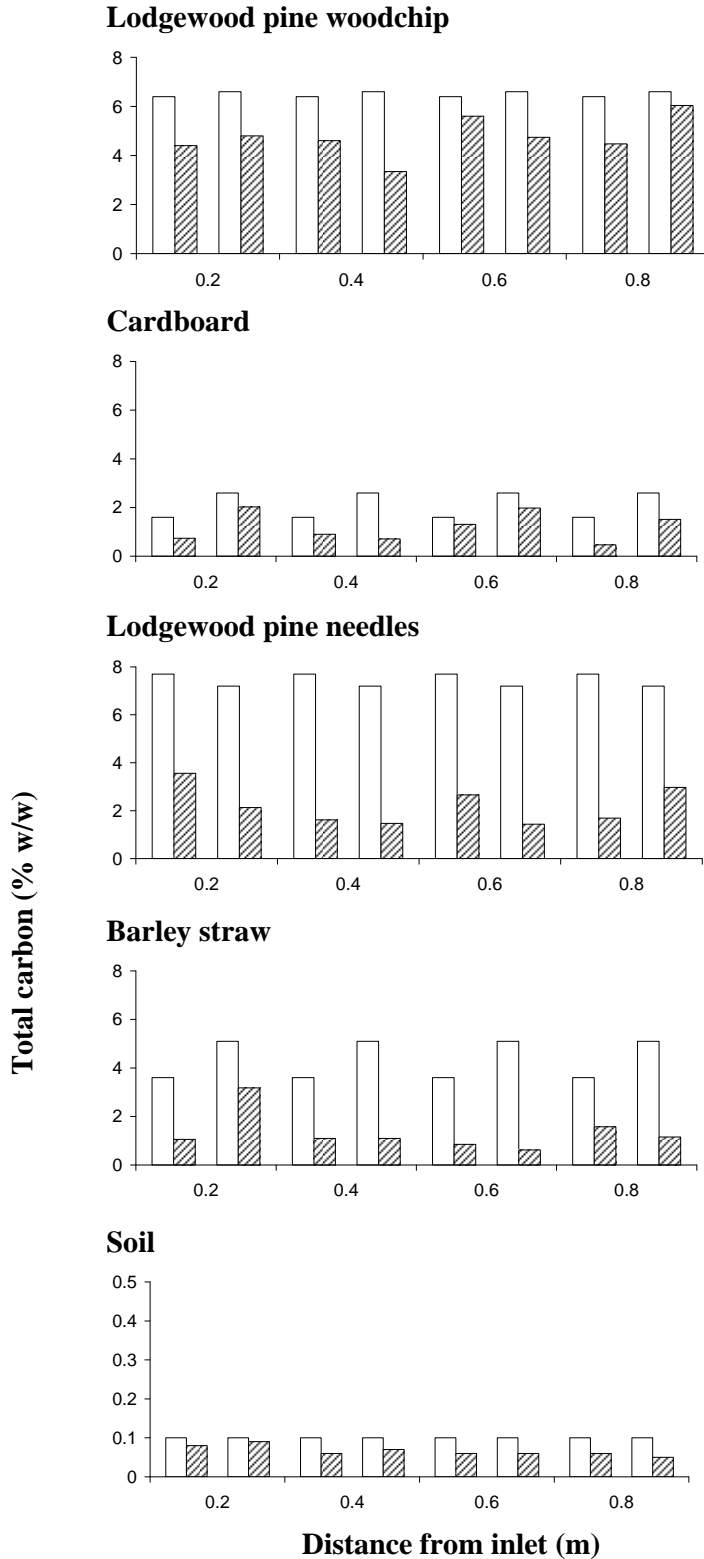
798 <sup>b</sup> Obtained from the sum of the sustainability indices (SIs) for each scenario

799  
800  
801  
802  
803  
804  
805  
806  
807  
808  
809  
810  
811  
812  
813  
814  
815



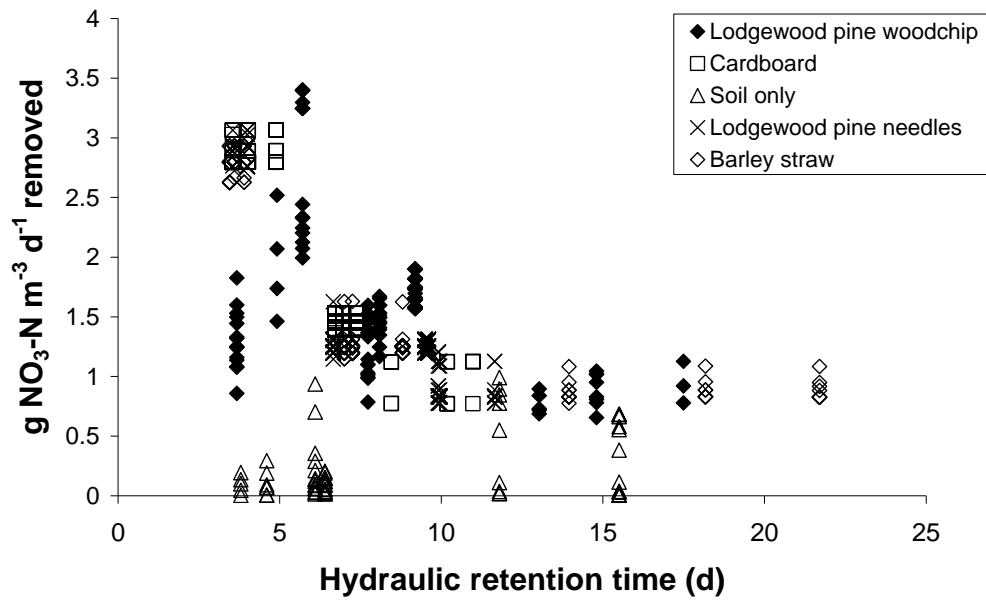
816  
817  
818  
819  
820

Figure 1. Influent and effluent nitrate concentrations and operation boundaries for each media. Open square = Column 1 effluent; Open triangle = Column 2 effluent; Open circle = Column 3 effluent; Closed diamond = influent  $\text{NO}_3^-$ -N concentration. Vertical lines represent the three hydraulic loading rates: 3, 5 and  $10 \text{ cm d}^{-1}$



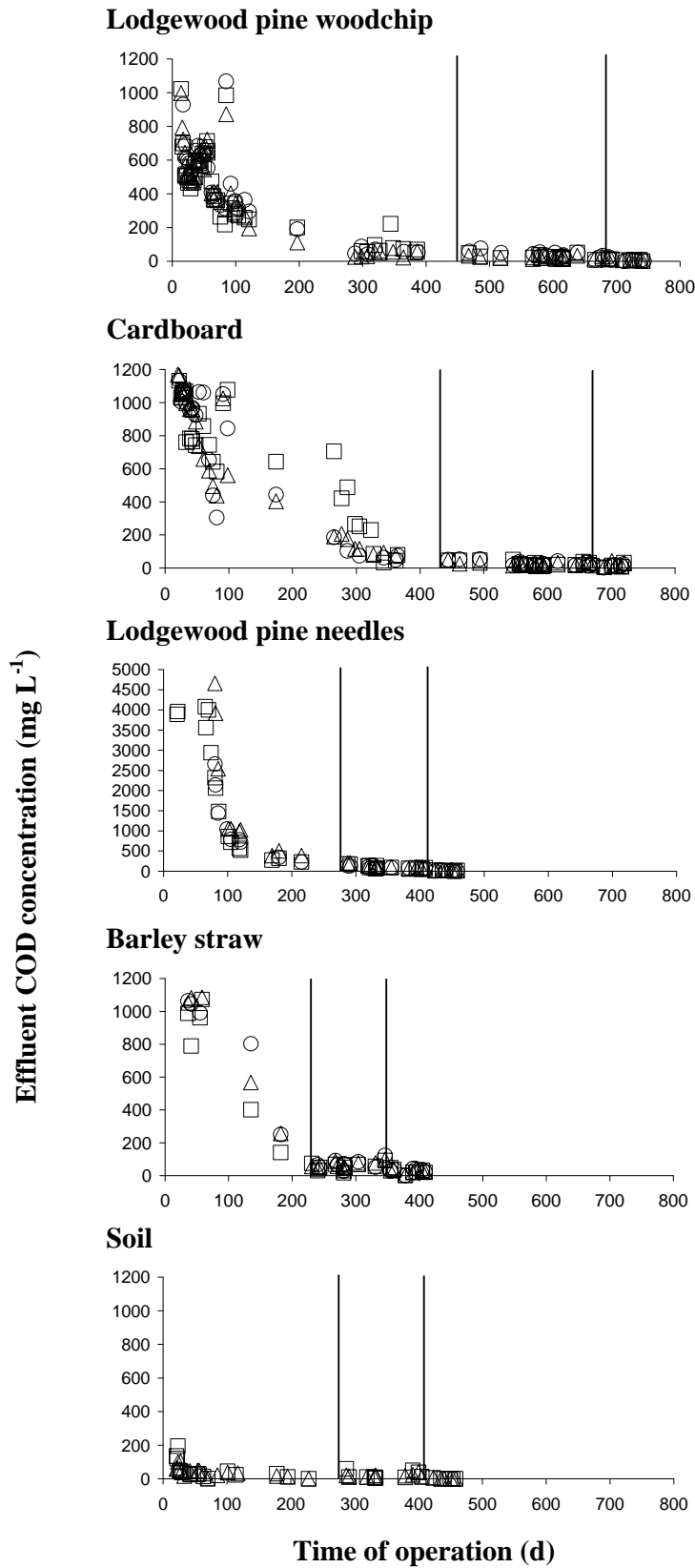
822 Figure 2. Total carbon, expressed as a % of total carbon per dry weight of material  
 823 (soil + filter media) in each 0.2 m depth of the bioreactors (n=2) at the start and end of  
 824 the study. White boxes = total carbon (%w/w) at the start of the study. Hatched boxes  
 825 = total carbon (%w/w) at the end of the study.

826  
827  
828  
829



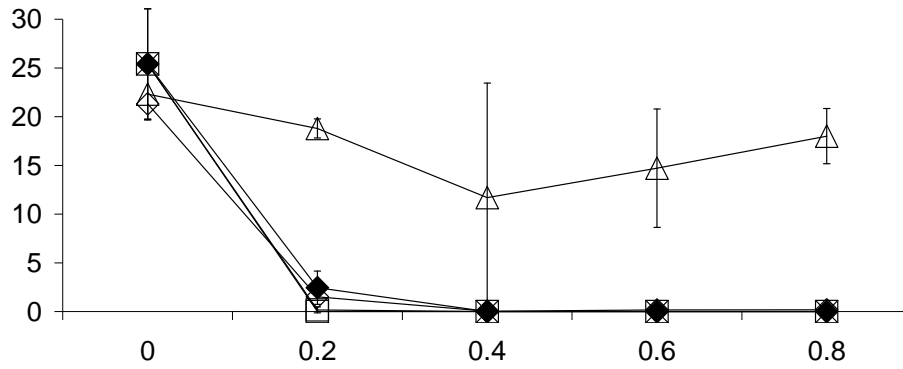
830  
831  
832  
833  
834  
835  
836  
837  
838  
839  
840  
841  
842  
843  
844  
845  
846  
847  
848  
849  
850  
851  
852  
853  
854  
855  
856  
857  
858

Figure 3. Relationship between hydraulic retention time (d) and nitrate-N removed (g NO<sub>3</sub>-N m<sup>-3</sup> d<sup>-1</sup>).

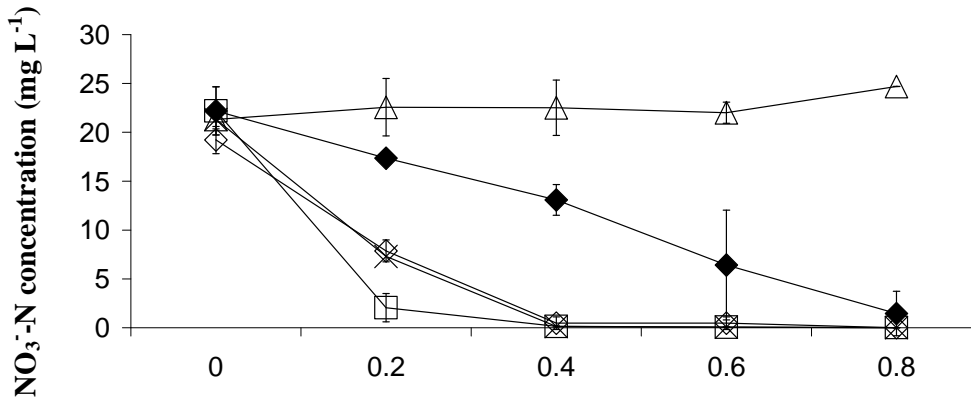


859 Figure 4. Effluent COD concentrations and operation boundaries for each media. Open square =  
 860 Column 1; Open triangle = Column 2; Open circle = Column 3. Vertical lines represent the three  
 861 hydraulic loading rates: 3, 5 and 10 cm d<sup>-1</sup>.

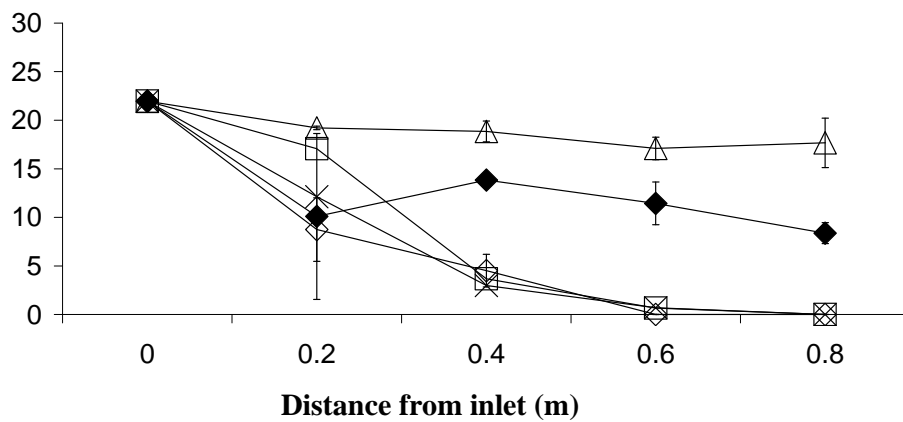
**Hydraulic loading rate: 3 cm d<sup>-1</sup>**



**Hydraulic loading rate: 5 cm d<sup>-1</sup>**



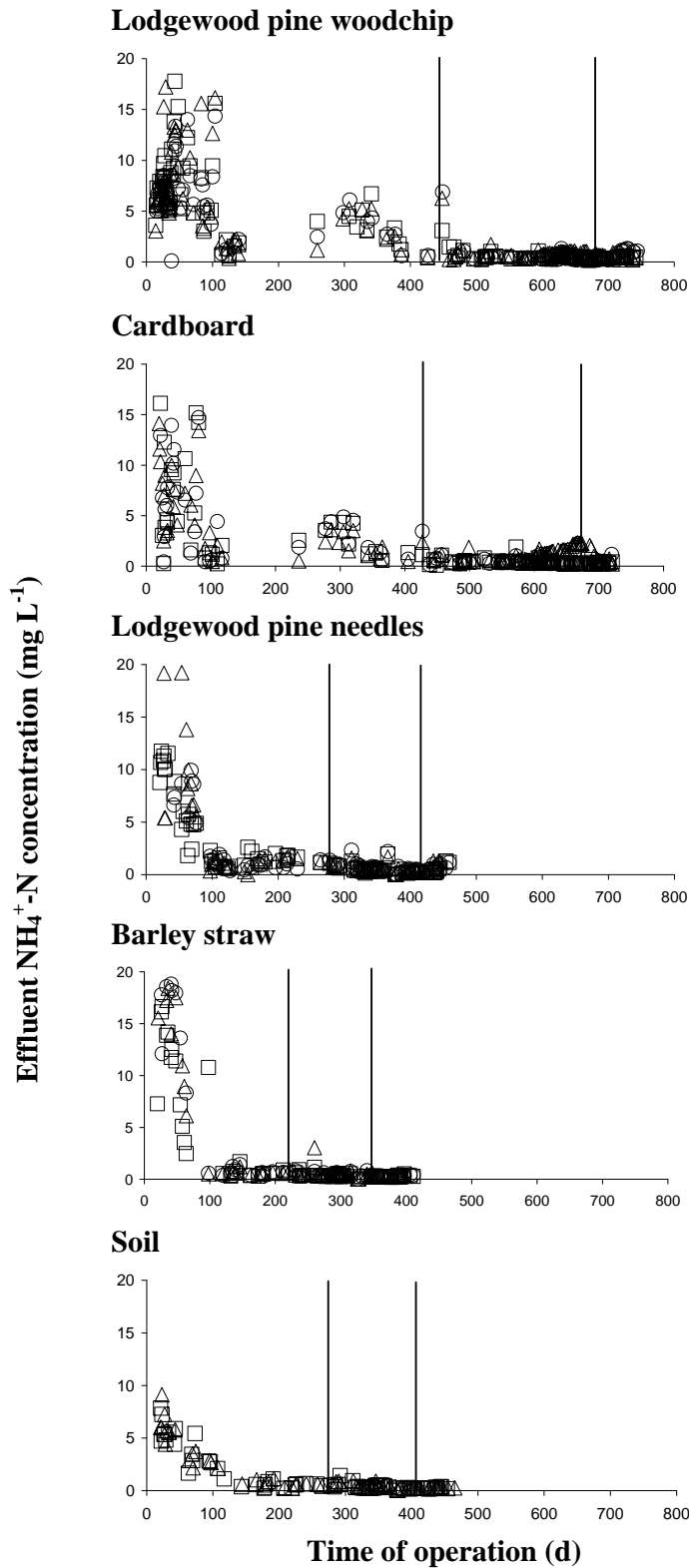
**Hydraulic loading rate: 10 cm d<sup>-1</sup>**



- ◆ Lodgewood pine woodchip
- Cardboard
- × Lodgewood pine needles
- ◇ Barley straw
- △ Soil only

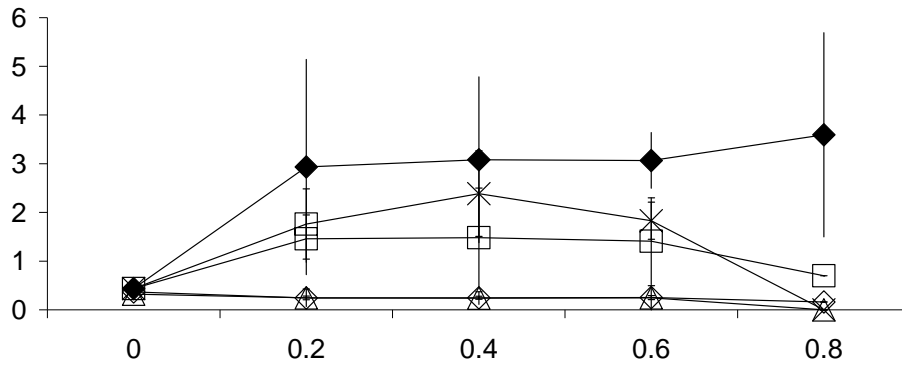
863  
864  
865  
866  
867

Figure 5. Average concentration of nitrate in one representative bioreactor containing each media during operation at hydraulic loading rates of 3, 5 and 10 cm d<sup>-1</sup>.

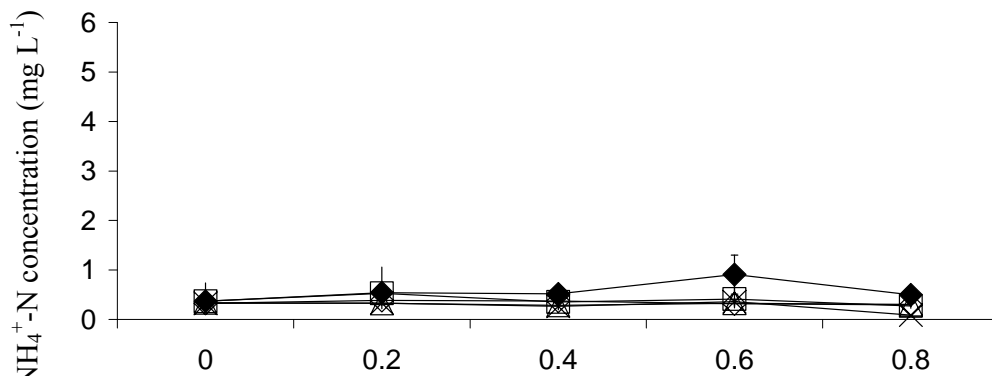


868 Figure 6. Effluent ammonium-N concentrations and operation boundaries for each  
 869 media. Open square = Column 1; Open triangle = Column 2; Open circle = Column  
 870 3. Vertical lines represent the three hydraulic loading rates: 3, 5 and 10 cm d<sup>-1</sup>.  
 871  
 872

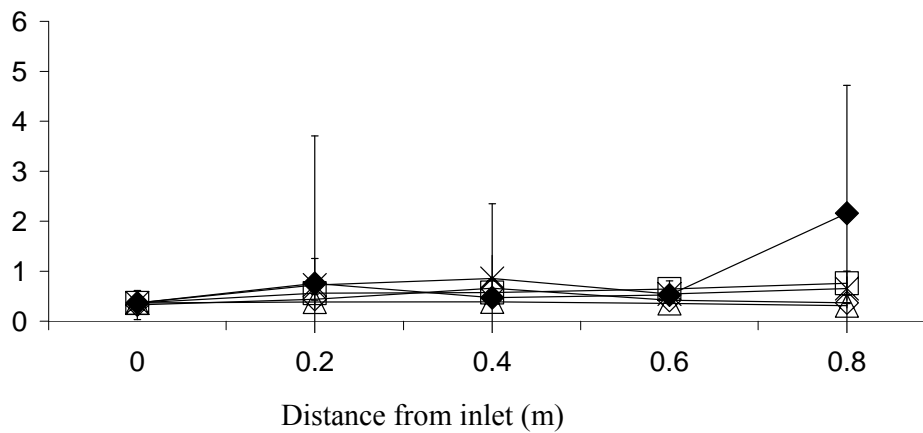
**Hydraulic loading rate: 3 cm d<sup>-1</sup>**



**Hydraulic loading rate: 5 cm d<sup>-1</sup>**



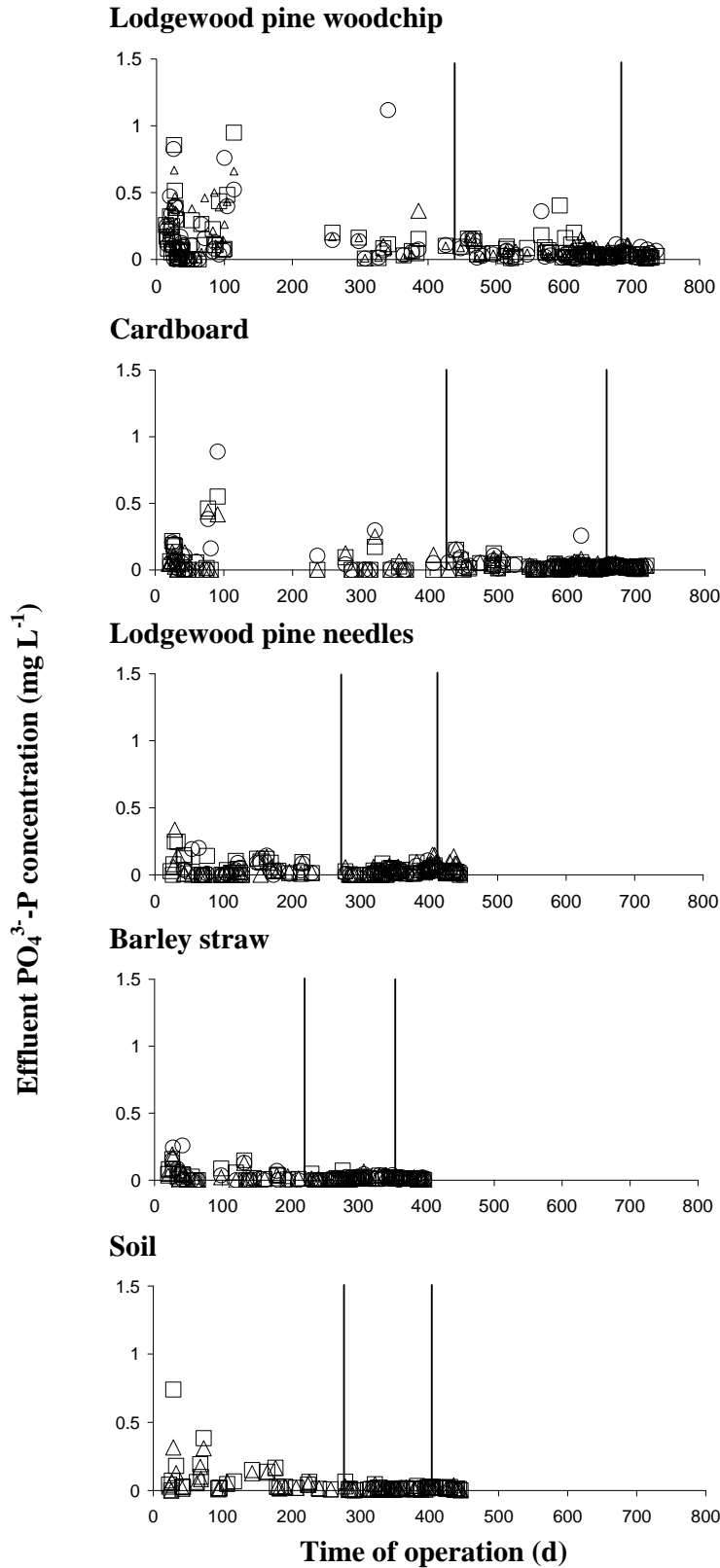
**Hydraulic loading rate: 10 cm d<sup>-1</sup>**



- ◆ Lodgewood pine woodchip
- Cardboard
- × Lodgewood pine needles
- ◇ Barley straw
- △ Soil only

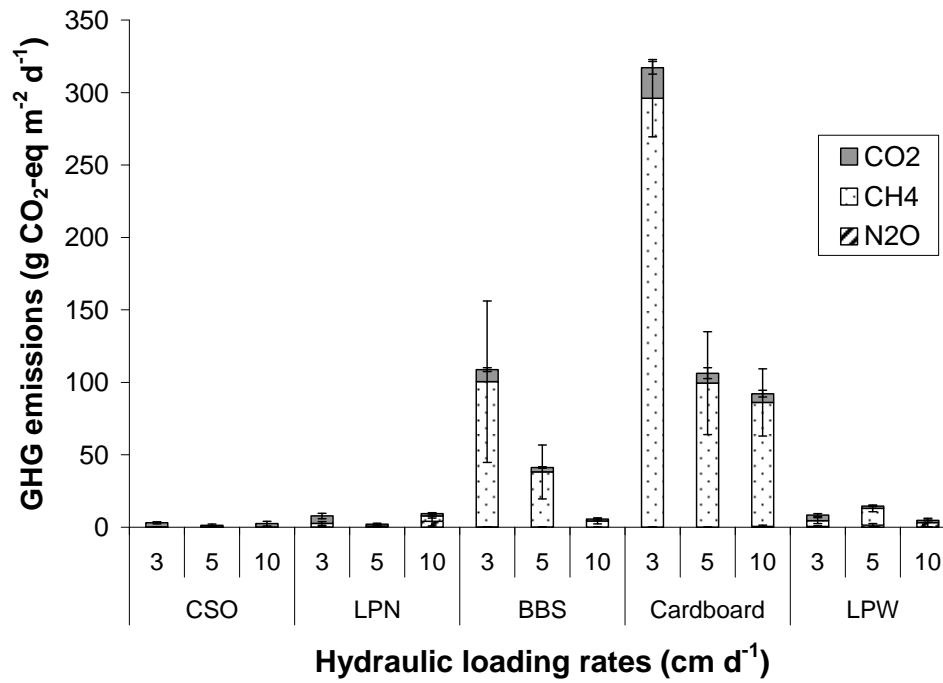
873  
874  
875  
876  
877

Figure 7. Average concentration of ammonium-N in one representative bioreactor containing each media during operation at hydraulic loading rates of 3, 5 and 10 cm d<sup>-1</sup>.



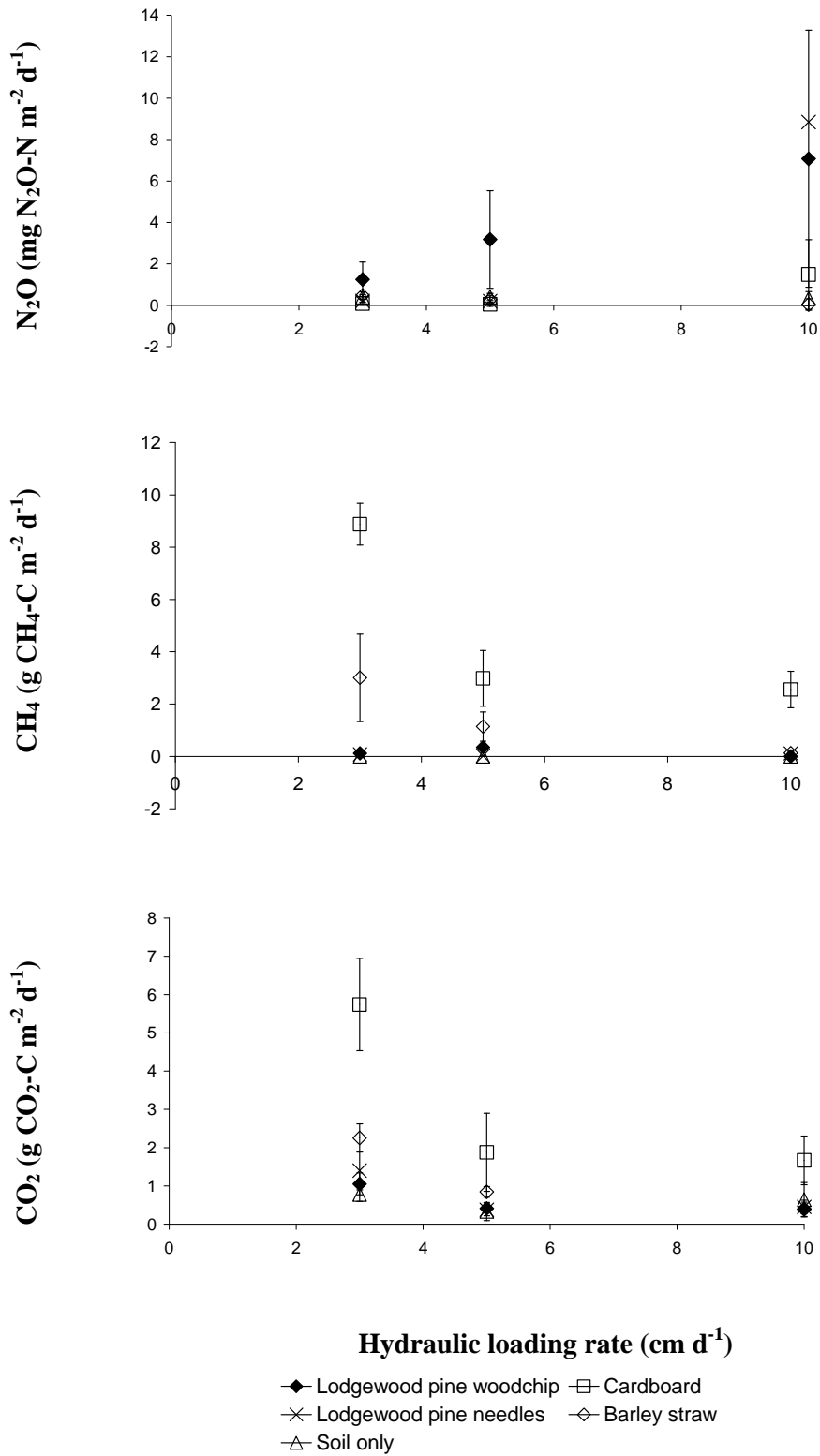
879 Figure 8. Effluent ortho-phosphorus concentration and operation boundaries for each media. Open  
 880 square = Column 1; Open triangle = Column 2; Open circle = Column 3. Vertical lines represent the  
 881 three hydraulic loading rates: 3, 5 and 10 cm d<sup>-1</sup>.

882  
883  
884



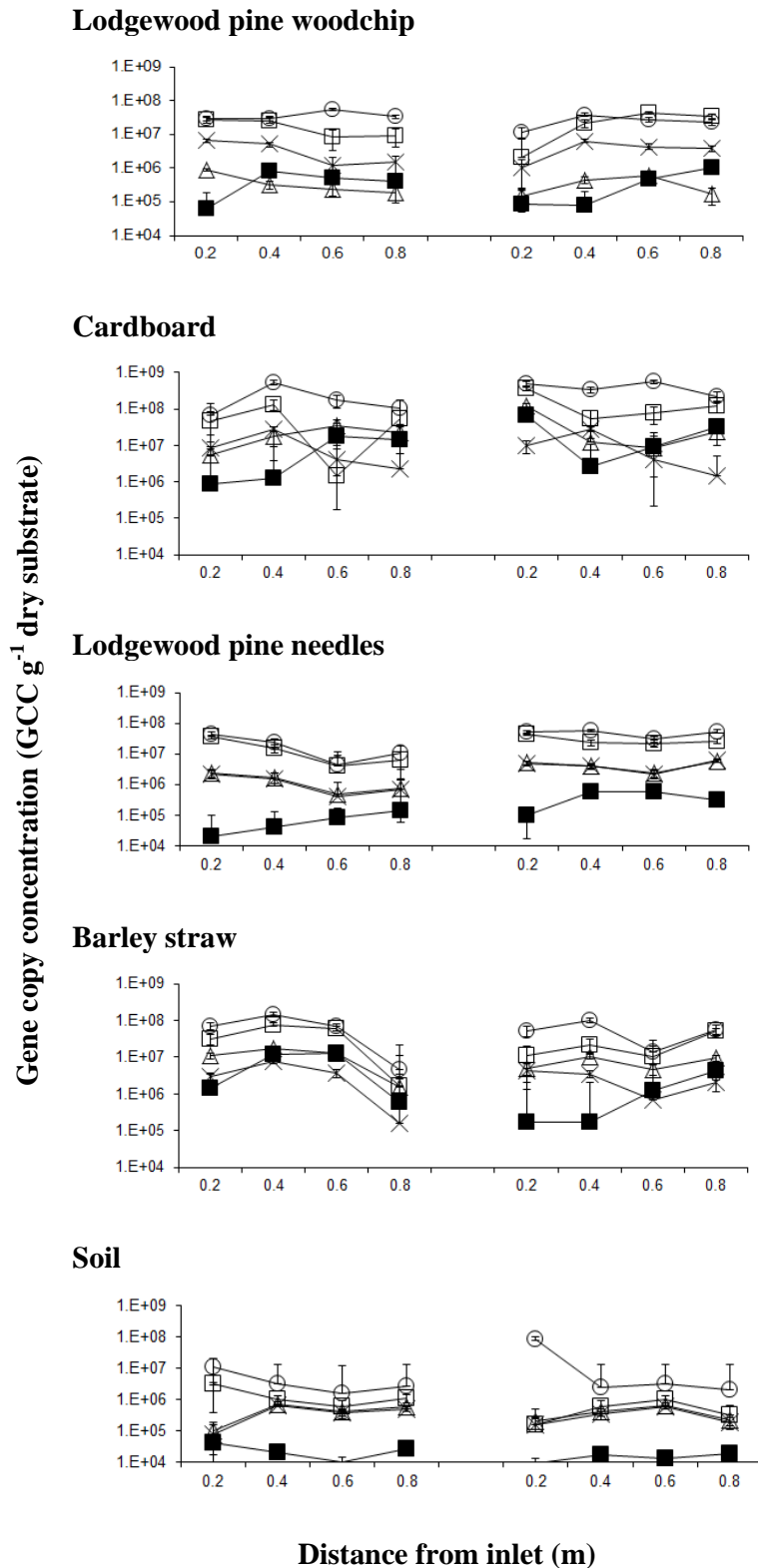
885  
886  
887  
888  
889  
890  
891  
892  
893  
894  
895  
896  
897  
898  
899  
900  
901  
902  
903  
904  
905  
906  
907  
908  
909  
910  
911  
912

**Figure 9.** Mean emissions of greenhouse gas (nitrous oxide (N<sub>2</sub>O), methane (CH<sub>4</sub>) and carbon dioxide (CO<sub>2</sub>)) emissions (± standard error), expressed as CO<sub>2</sub> equivalents per unit surface area per day.



914  
915  
916  
917

**Figure 10.** Relationship between hydraulic loading rate and emissions ( $\pm$ standard error) in the denitrifying bioreactors.



918 **Figure 11.** Variation in gene copy concentration (GCC) of *nirK* (open triangle), *nirS* (open square),  
 919 *nosZ* (cross hairs) and archaeal (closed square) and bacterial 16S rRNA (open circle) obtained from  
 920 sampling ports located at distances of 0.2, 0.4, 0.6 and 0.8 m from the base in two arbitrary sets of  
 921 lodgewood pine woodchip, cardboard, lodgepole pine needles, barley straw and soil-only bioreactors  
 922 (NTC undetected for each respective assay). Standard errors are indicated for each separate Q-PCR  
 923 subgroup (n = 3).

